



Physical cleaning efficacy of hollow fiber nanofiltration membranes in drinking water applications

Analita Payant^a, Pierre R. Bérubé^b, Benoit Barbeau^{a,*}

^aIndustrial-NSERC Chair in Drinking Water, École Polytechnique de Montréal, Département des Génies Civil, Géologique et des Mines, CP 6079, succ. Centre-Ville, Montréal, QC, H3C 3A7, Canada, Tel. +1 (514) 340-4711 Ext. 2988; Fax: +1 (514) 340-5918; email: benoit.barbeau@polymtl.ca (B. Barbeau), Tel. +1 (514) 340-4711 Ext. 2975; Fax: +1 (514) 340-5918; email: analita.payant@polymtl.ca (A. Payant)

^bUniversity of British Columbia, Department of Civil Engineering, Vancouver, BC, V6T 1Z4, Canada, Tel. +1 (604) 822-5665; Fax: +1 (604) 822-6901; email: berube@civil.ubc.ca

Received 6 April 2016; Accepted 21 August 2016

ABSTRACT

The aim of this research was to study the role of hydrodynamic conditions on the efficacy of physical cleaning (rinsing and backwash steps using water and/or air) for hollow fiber nanofiltration (HFNF). Bench-scale inside/out HFNF membranes, as well as hollow fiber ultrafiltration (HFUF) tested as a reference, were fouled in dead-end (DE) or crossflow (CF) operation with synthetic water consisting of a mixture of sodium alginate and kaolin clay. Six physical cleaning strategies (3 average water velocities ranging from 0.06 to 0.27 m/s × 2 air velocities (0.51 m/s or none) were tested after triplicate filtration cycles. The physical cleaning efficacy was assessed by performing a mass balance recovery of the alginate and kaolin fed in the system. No difference in physical cleaning efficacy was observed for the two types of membranes in CF operation. High water velocity and air addition improved the physical cleaning efficacy. During CF operation, alginate and kaolin were mostly (75%–86%) recovered in the concentrate as opposed to physical cleaning waters (below 8%). Fouling management achieved by a combination of physical cleaning and CF operation was superior to what was achieved in DE operation with physical cleaning. For HFNF, the energy costs for physical cleaning were marginal compared with those associated with CF operation, but can be reduced by using a shorter backwash duration and air-assisted forward flush.

Keywords: Hollow fiber nanofiltration; HFNF; Dual-phase flow; Backwash; Energy consumption; Drinking water

1. Introduction

As opposed to ultrafiltration (UF), nanofiltration (NF) membranes can retain a significantly higher fraction of natural organic matter (NOM) including disinfection by-product precursors as well as trace organic contaminants, whether regulated (e.g., pesticides or algae toxins) or of emerging concern (e.g., endocrine disruptors or personal care products). However, the expansion of NF in the water industry has been limited by its relatively low flux, high energy consumption

and fouling propensity compared with low-pressure membranes (e.g., microfiltration and UF) [1]. Currently, NF modules are typically configured as spiral-wound elements, which cannot effectively be physically cleaned. In addition, many NF membrane materials (e.g., polyamide) cannot be cleaned with oxidants such as hypochlorite solutions, limiting the ability to control microbial and organic fouling. Therefore, adequate pre-treatment prior to spiral-wound NF is essential for the successful application of this technology [2]. The recent development of commercial hollow fiber NF membranes (HFNF), which can be physically cleaned, as well as chemically cleaned with oxidants such as hypochlorite

* Corresponding author.

solutions (e.g., X-Flow HFW1000), represents a significant innovation for the water industry. The possibility to reduce the extent of pre-treatment required before HFNF could expand the application of this technology.

Membrane fouling has been investigated under various angles such as the water characteristics [3–5], the membrane composition [6–8] and operation conditions [9,10]. The present study focuses on physical (hydraulic) cleaning, which is an important strategy for managing fouling of hollow fiber membranes. In hollow fiber UF (HFUF), this is typically achieved by a combination of steps including single or dual-phase (i.e., air/water) rinsing (i.e., forward flush) and backwashes. To the best of our knowledge, no studies have assessed if physical cleaning strategies commonly used for HFUF would also be applicable for HFNF membranes. Considering the current knowledge on fouling mitigation, it is expected that the use of air could play an important role to mitigate fouling in HFNF systems. Air addition in outside/in HFUF systems during permeation is recognized as an effective approach to reduce fouling [11,12]. The efficacy of fouling control has been correlated to wall shear stress induced by rising air bubbles and fiber movement. Air addition (i.e., dual-phase air/water for feed flow) was also demonstrated to be effective at reducing fouling for inside/out HFUF membranes [13–16]. The flow pattern plays a key role with slug flow being considered as the most effective for fouling mitigation. Once again, efficacy was correlated with the shear induced by the dual-phase flow [14,15]. With respect to HFNF, dual-phase flow obtained by injecting air during crossflow (CF) operation was also reported to increase permeate flux while reducing the concentration-polarization induced by the synthetic water tested (7–12 g/L $\text{MgSO}_4 \cdot 7\text{H}_2\text{O}$) [17].

As a second option, dual-phase flow can also be used during physical cleaning rather than during permeation. The efficacy of physically assisted air cleaning of HFUF has been shown for dead-end (DE), outside/in [18] and inside/out [19] operation. In the last case, the authors identified air-assisted backwash (BW) followed by a final rinsing step as the most cost-effective strategy. In a subsequent study, they recommended a mass balance analysis as the most sensitive method to estimate physical cleaning efficacy (rather than analyzing permeability loss) [20].

Although it is anticipated that air-assisted physical cleaning will also be beneficial to mitigate fouling in HFNF membranes, there are several important differences in their operation compared with that of HFUF membranes that suggest differences in the efficacy of physical cleaning strategies for HFNF and HFUF. First, commercially available HFNF membranes are operated with CF, while HFUF membranes are typically operated in DE mode for drinking water applications. CF is useful to reduce NOM concentration-polarization [21] and limit cake accumulation [22]. Second, the operating flux of HFNF (10–25 LMH) is significantly lower than that of HFUF (50–100 LMH) systems, which implies lower foulants advection to the membrane. Third, NOM retention is higher in HFNF due to the lower molecular weight cut-off of these membranes. Consequently, the objectives of this research were to: (i) compare the efficacy of various physical cleaning strategies for HFNF membranes, (ii) evaluate the impact of operating conditions on physical cleaning strategies, and (iii) explore the hydrodynamic and economic benefits of dual-phase physical cleaning strategies.

2. Materials and methods

2.1. Membrane modules

The experiments were carried out using bench-scale inside/out HFUF and HFNF membranes (Pentair, X-Flow®). The two bench-scale modules had an identical filtration surface (0.07 m²), module length (30 cm) and inner fiber diameters (0.8 mm). The molecular weight cut-offs of the HFUF and HFNF membranes are 150 and 1 kDa, respectively. The HFUF membrane is composed of a Polyethersulfone (PES)/Polyvinyl Pyrrolidone (PVP) blend, and the HFNF material is a modified PES [23]. Although a 1-kDa molecular weight cut-off (MWCO) could be considered either as a loose NF or a tight UF membrane, we will refer to it as a NF membrane throughout this paper.

2.2. Synthetic waters

All fouling assays were conducted using synthetic waters, which characteristics were selected to mimic surface water. In order to achieve this objective, ultrapure water (Milli-Q®) was amended with kaolin clay (a particulate contaminant), sodium alginate (a biopolymer) and sodium bicarbonate (to add alkalinity). The model water contained 15 mg/L of kaolin clay, 5 mg C/L of sodium alginate (Sigma-Aldrich, USA, CAS: 9005-38-3) and sodium bicarbonate (50 mg CaCO_3/L). The final model water pH was adjusted to 7.0 with HCl and had a turbidity of 16.4 NTU. The kaolin was added to the water immediately before the start of the filtration tests, and it was previously placed in an ultrasound bath to ensure an even distribution of particle sizes for all assays. The median kaolin particles size was estimated to be 9.6 μm by sequential filtration. The synthetic water without kaolin was subjected to size exclusion chromatography with organic carbon detection (LC-OCD). The sodium alginate in solution produced a narrow peak at 54,500 Da.

2.3. Experimental setup

Fig. 1 illustrates the experimental setup, which includes a feed pump (magnetic gear, BVP-Z, Ismatec, Germany) and peristaltic pump (Masterflex L/S, Cole-Parmer, Canada) installed on the permeate side to maintain constant flux during filtration. On-line pressure (PX409-100GUSB and PX409-030GUSB, OMEGA, Canada) is monitored with OMEGA software. Flow is calculated by gravimetry (with a precision of ± 0.01 mg). The temperature is monitored by a sensor located in the feed water tank and was kept at $20^\circ\text{C} \pm 0.5^\circ\text{C}$ using a cooling system (1171PD, VWR, USA). The setup also includes a pressurized air inlet connected to the feed line. The air flow rate was measured with a rotameter (Gilmont GF-1360, Cole-Parmer, Canada) and validated with a gas bubble flow meter. Physical cleaning waters were collected from the drainage line.

2.4. Operation mode and physical cleaning protocols

Every filtration experiments consisted of a series of three permeation cycles at constant flux (20 LMH), each followed by a physical cleaning. Each physical cleaning was initiated after that 20 L/m² of permeate had been filtered. The filtration experiments were conducted either under DE or under CF operation (at 0.5 m/s). Under CF operation, flow rates

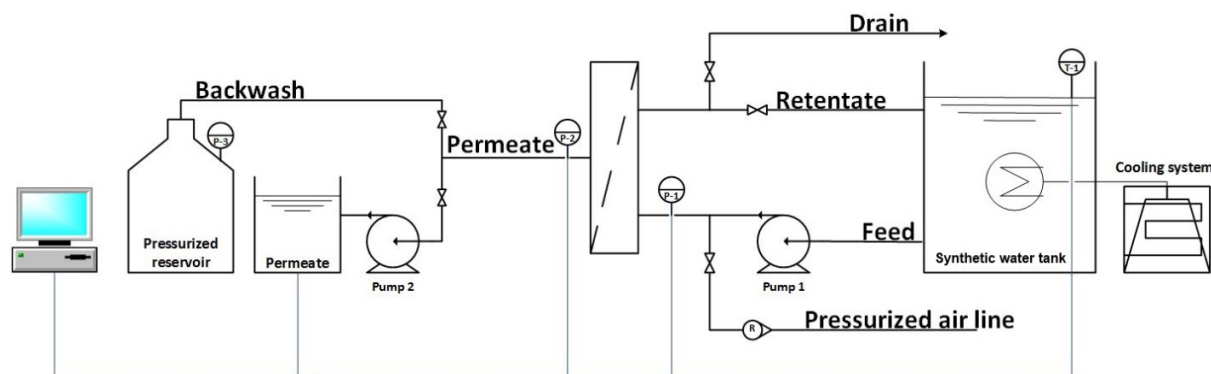


Fig. 1. Experimental setup.

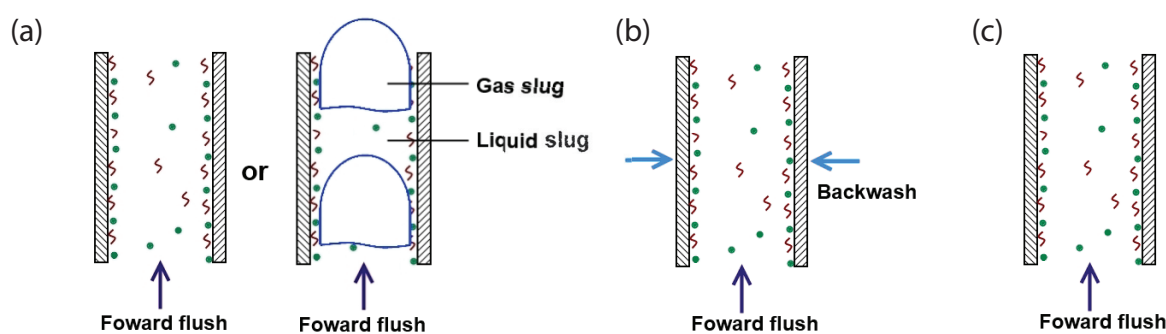


Fig. 2. Physical cleaning steps: (a) forward flush with or without air; (b) backwash with forward flush; and (c) forward flush without air.

Table 1
Physical cleaning protocols

Protocols	Cleaning steps	Duration (s)	Water velocity (m/s)	Air velocity (m/s)	Average water velocity ^a (m/s)
1	Forward flush with or without air	55	0.05	0.51	0.06
	Backwash + forward flush	60	0.08	0.00	
	Forward flush	55	0.05	0.00	
2	Forward flush with or without air	20	0.11	0.51	0.16
	Backwash + forward flush	25	0.23	0.00	
	Forward flush	10	0.11	0.00	
3	Forward flush with or without air	20	0.17	0.51	0.27
	Backwash + forward flush	25	0.38	0.00	
	Forward flush	10	0.17	0.00	

^aTime-weighted average.

were 84 L/h (feed), 1.4 L/h (permeate = 2%) and 82.6 L/h (concentrate = 98%). The recoveries for DE and CF operation are 98% and 76%, respectively.

Six different physical cleanings strategies were investigated. All strategies involved three successive steps (Fig. 2). The first step consisted of a forward flush using synthetic feed water with or without air addition (Fig. 2(a)). The second step consisted of a forward flush with a BW (Fig. 2(b)). A synthetic permeate, consisting of the model water without sodium alginate or kaolin, was used as the BW water. The

third step is a forward flush without air addition (Fig. 2(c)). After the third step, the filtration resumed. Physical cleaning water and air velocities were adapted from manufacturer recommendations and typical conditions prevailing in the water industry. Note that the manufacturer did not recommend air injection during the forward flush for HFNF membranes. The duration of air injection was set to 10 s at 0.51 m/s (0.088 m³/h) while the BW flux was set to 40 LMH (2.8 L/h), i.e., two times the HFNF permeate flux. A summary of the physical cleaning characteristics is presented in Table 1.

Between filtration experiments, the membranes were cleaned with Milli-Q water, a sodium hydroxide solution (1 mM NaOH) and a hydrochloric acid solution (1 mM HCl) prior to storage in the dark in a NaHSO₃ solution (200 mg/L) at 4°C. The HFNF was first backwashed with ultrapure water and then soaked with recirculation for both chemical solutions (with ultrapure rinsing between the steps) while the HFUF was first backwashed with ultrapure water and then with the cleaning solutions (with ultrapure rinsing between the steps) as recommended by manufacturer. Permeability recovery by CIP was always 100% throughout the project. Finally, membrane integrity was confirmed prior each assay by performing a pressure-hold tests ($P_o = 15$ psig).

2.5. Assessment of physical cleaning efficacy

During this study, the permeability was always stable while operating in CF. Therefore, physical cleaning efficacy was not assessed using permeability recovery because this approach did not provide enough sensitivity, a conclusion that had also be drawn by Remize, et al. [20]. As an alternative, a mass balance analysis was performed to assess the recoveries of foulants. The kaolin and alginate masses were measured independently. The kaolin concentration in the waters (initial feed, concentrate and physical cleaning waters) was indirectly measured using absorbance (DR 5000 UV-Vis spectrophotometer, HACH, Canada) at 861 nm in a 1-cm spectrophotometric cell (linearity relationship between 0 and 50 mg/L, $R^2 = 0.999$). The detection limit was estimated to be 0.6 mg/L. The presence of sodium alginate did not impact the measurements. The sodium alginate concentration was determined using a TOC-analyzer (Sievers 5310 C Laboratory TOC Analyzer, GE®). The detection limit was estimated to be 0.07 mg C/L.

The physical cleaning efficacy was evaluated by calculating the fraction of foulants recovered (%) using Eq. (1) in which the kaolin and alginate loads were summed up as an initial analysis showed that similar removal trends were observed for both foulants. Physical cleaning efficacy among cleaning protocols were compared statistically by conducting an Analysis of Variance (ANOVA) (with interactions) with Statistica 10.0 (Statsoft, USA).

Fraction of foulants recovered (%)

$$= \left(\frac{\text{Physical cleaning mass}}{\text{Feed mass} - \text{Permeate mass}} \right) \times 100 \quad (1)$$

2.6. Hydrodynamic conditions

In order to assess the role of hydrodynamic conditions on physical cleaning efficacy, theoretical shear conditions and dual-phase Reynolds number inside the fiber were calculated for each cleaning protocol step. For both parameters, maximum and time-weighted averages were calculated.

2.6.1. Dual-phase Reynolds number

Reynolds number was investigated based on the homogenous-flow model where the dual-phase is considered as a single-phase flow with average properties of the mixture [24].

$$Re_m = \frac{\rho_m U_m D}{\mu_m} \quad (2)$$

where Re_m is the mixture Reynolds number; D is the fiber diameter (m); ρ_m is the mixture density (kg/m³); μ_m is the mixture dynamic viscosity (Pa.s) and U_m is the mixture velocity (m/s), which is defined as follows:

$$U_m = U_G + U_L \quad (3)$$

where U_L and U_G are, respectively, the liquid and gas phase (m/s).

2.6.2. Shear stress

For single-phase flows, the wall shear stress (τ_{wall}) can be calculated from the Darcy–Weisbach equation [25]:

$$\tau_{\text{wall}} = \frac{f_f U_L \rho_L}{2} \quad \text{where } f_f = \frac{f_D}{4} \quad (4)$$

where f_f is a friction factor correlated to the Darcy friction factor f_D , which is defined by Eq. (5) for laminar flow conditions ($Re < 2,000$):

$$f_D = \frac{64}{Re} \quad (5)$$

The dual-phase flow wall shear stress is calculated from the pressure loss (ΔP) by friction along the fiber length (ΔL) according to:

$$\tau_{\text{wall}} = \frac{D \Delta P}{4 \Delta L} \quad (6)$$

The pressure loss was estimated using the separated flow model of Lockhart–Martinelli [26]. The model proposes correlations between pressure loss for each of the phases (using a multiplier factor Φ_L^2) and an empirical parameter (X). The two pressure losses (air and water) are calculated separately with the same equation:

$$\left[\frac{\Delta P}{\Delta L} \right]_G = \frac{f_D \rho_G U_G^2}{2D} \quad \text{and} \quad \left[\frac{\Delta P}{\Delta L} \right]_L = \frac{f_D \rho_L U_L^2}{2D} \quad (7)$$

$$\left[\frac{\Delta P}{\Delta L} \right]_L = X^2 \left[\frac{\Delta P}{\Delta L} \right]_G \quad (8)$$

$$\Phi_L^2 = 1 + \frac{C}{X} + \frac{1}{X^2} \quad (9)$$

A relationship is required to estimate the factor Φ_L^2 , the Chisholm equation [27] was used for this purpose. It includes an empirical factor (C) that can be calculated using the Mishima–Hibiki relationship, which was recently modified to take into account the surface tension (σ), an important parameter for flow in small tubes [28].

$$C = 21(1 - e^{-0.674/L\sigma^*}) \quad (10)$$

$$Lo^* = \frac{\sigma}{\sqrt{g(\rho_L - \rho_G)D^2}} \quad (11)$$

Eq. (10) is applicable for hydraulic diameters ranging from 0.014 to 6.25 mm. The coefficient of 0.674 is recommended for adiabatic laminar liquid–gas mixtures [28].

2.7. Energy consumption

Energy consumption was calculated in order to compare cleaning protocols with respect to their cleaning efficacy, the operating costs and the volume of wastewaters produced. Calculations were made for an industrial module using the following assumptions:

- industrial NF module: filtration surface of 40 m² and 1.54 m fiber length,
- NF membrane permeability: 8.3 LMH/bar at 20°C,
- two stages of filtration (2 + 1 configuration) with a total recovery of 85%,
- flux: 20 LMH,
- operating feed pressure: 2.4 bar (35 psig),
- filtration cycles of 1 h followed by a physical cleaning, and
- BW: 40 LMH at 4.8 bar (70 psig).

3. Results

3.1. Physical cleaning efficacy for crossflow operation

To evaluate the efficacy of various physical HFNF cleaning strategies, each protocol and its variant (with or without air) were first tested in CF operation (0.5 m/s) at a constant flux of 20 LMH. Four of the six physical cleanings strategies (protocols 1 and 3 with and without air) were also evaluated on a HFUF membrane operated with the same conditions (0.5 m/s and 20 LMH).

The fractions of foulants recovered (*cf* Eq. (1)) by the various physical cleaning strategies considered are reported in Fig. 3. The fractions of foulants recovered were constantly low (<8%) because, under CF operation, most of the matter contained in the feed water did not accumulate on the membrane, but was present in the concentrate (75%–86%). An ANOVA analysis revealed that the water velocity, the addition of air as well as their synergistic interaction significantly impacted the physical cleaning efficacy ($p < 0.001$ in all three cases). The use of air and higher water velocities improved the fraction of foulants recovered by 2.5-fold compared with a low water velocity in the absence of air. Physical cleaning strategies with air recovered 1.4 to 1.7 times more foulants than equivalent physical cleaning strategies without air. The use of higher water velocities without air addition improved the fraction of foulants recovered by 1.4-fold compared with a low water velocity. The efficacy of the physical cleaning strategies was statistically equivalent for both the HFUF and HFNF membranes ($p = 0.78$).

3.2. Impact of operation mode: crossflow vs. dead-end

The most efficient cleaning protocol (protocol 3 with air addition) was tested on both HFNF and HFUF membranes operated in DE mode with a constant flux of 20 LMH and

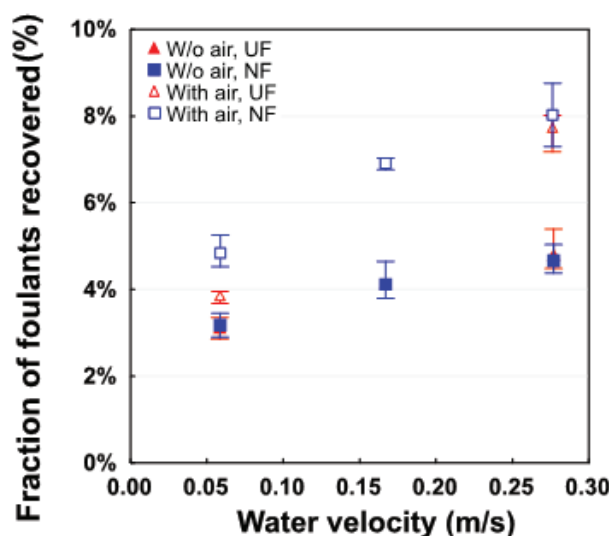


Fig. 3. Fractions of foulants (alginate and kaolin) recovered from physical cleaning for HFUF and HFNF membranes (flux 20 LMH and CF of 0.5 m/s; error bars provide the min-max deviations from triplicate filtration tests).

compared with those operated with CF. As opposed to CF operation, the fraction of foulants recovered in the physical cleaning waters was very high after DE operation since no matter was recovered in the concentrate. For example, the mass of foulants that accumulated on the membranes before physical cleaning can be calculated by subtracting the concentrate and permeate masses from the feed water mass. For DE and CF operation, the accumulation prior to the physical cleaning were 37.9 and 11.1 mg, respectively (a 3.4-fold difference). In order to compare the fraction of foulants recovered under both modes of operation, the fractions of alginate and kaolin recovered in the concentrate (75%–86%) were added to the fraction recovered during physical cleaning (<8%). Under this basis of comparison, the total fractions of foulants recovered were higher ($p < 0.01$) for CF than DE operation (Fig. 4(a)). For CF operation, the results were not statistically different for the HFUF and HFNF membranes ($p = 0.34$). However, when operating in DE mode, the total fraction of foulants recovered was lower for the HFNF than the HFUF ($p = 0.03$).

Our results can be compared with the work of Remize et al. [20], which evaluated the benefits of using air-assisted BW to clean inside-out HFUF membranes operated in DE. The average fraction of foulants recovered in BW waters increased from 36% to 87% with air injection. DE assays conducted during our study always included air-assisted cleaning. We calculated foulants recoveries of 83% (HFNF) or 88% (HFUF), which values are similar to the ones found by Remize et al. (even though their feed concentration was solely composed of 170 mg/L of bentonite) [20].

CF operation of HFNF has been reported to reduce permeate DOC concentrations in surface water applications [29]. However, in the present study, the mode of operation did not impact the permeate water quality. Permeate kaolin concentrations were consistently below the detection limit while alginate concentrations were not statistically different for DE and CF operation (Table 2, $p = 0.97$). This is possibly related

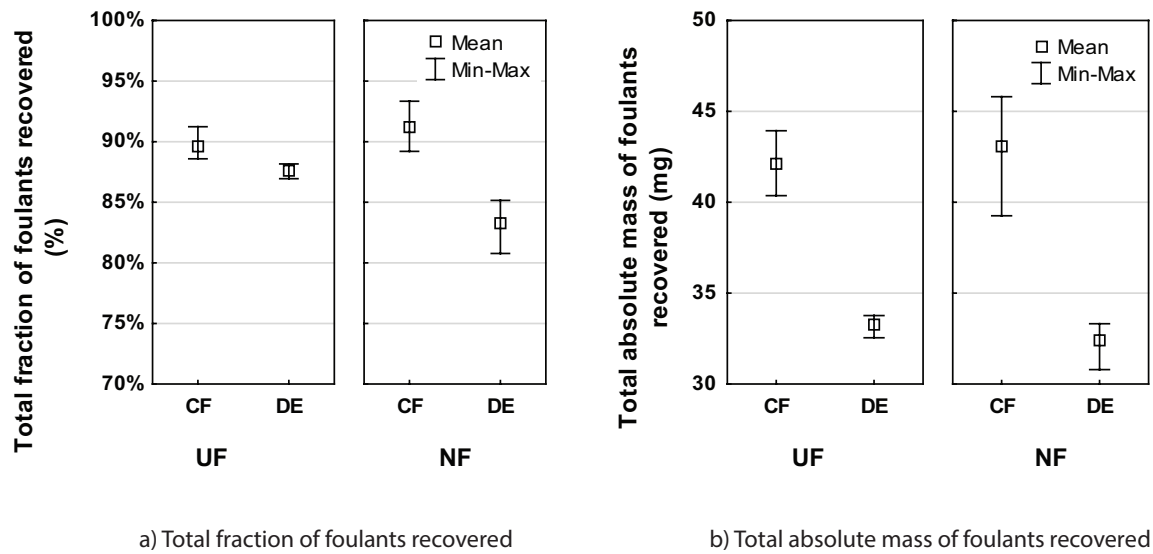


Fig. 4. Impact of operation mode on physical cleaning efficacy (flux 20 LMH, CF of 0.5 m/s vs. DE; physical cleaning (protocol P3 with air): average water velocity of 0.27 m/s with air addition 0.51 m/s; masses of foulants fed to the membranes in CF and in DE were 52 and 39 mg, respectively).

Table 2
Alginate concentration in permeate vs. membrane porosity and operation mode

Membranes	Operation mode	Alginate concentration in permeate (mg C/L)	
		Average	Standard deviation
NF	Crossflow	0.31	0.10
	Dead-end	0.32	0.07
UF	Crossflow	0.46	0.14
	Dead-end	0.45	0.10

to the molecular weight of alginate (i.e., 55 kDa), which is too high to generate substantial concentration-polarization [30]. The alginate concentration was significantly lower in the permeate from the HFNF than from the HFUF (Table 2, $p = 0.001$). Because the alginate retention between the two membranes was statistically different, the physical cleaning efficacy was also investigated by comparing the total absolute mass of foulants recovered (Fig. 4(b)). The total absolute masses of foulants recovered were in agreement with the total fractions of foulants recovered, except for the efficacies of HFNF and HFUF operated in DE mode, which were not statistically different ($p = 0.60$).

In summary, the mode of operation (i.e., CF vs. DE) was the most important factor affecting the efficacy of physical cleaning. This is because CF operation can be considered as a continuous shear effect during permeation. For CF operation, most of the kaolin and alginate contained in the feed was present in the concentrate. This implies that, for an equivalent feed load, the permeation time of a filtration cycle for HFNF membranes can be greater for CF compared with DE operation. The manufacturer of the HFW1000 (HFNF)

recommends that physical cleaning be performed every 60–120 min of permeation. This frequency is about 3 times longer than what is typically recommended for HFUF in DE mode (15–60 min) but is consistent with the reduced accumulation of foulants that we measured during this project for the CF-operated HFNF membrane (3.4-fold less foulants was accumulated on the membrane in CF as compared with DE operation). A lower physical cleaning frequency offers the benefits of reducing downtime for physical cleaning, lower wastewaters production and energy costs. The physical cleaning frequency is expected to depend on source water characteristics, CF velocity and targeted water recovery.

3.3. Shear and Reynolds number as indicators of physical cleaning efficacy

As physical cleaning protocols involve numerous steps with variable hydrodynamic conditions, it was of interest to test if one indicator could correctly predict physical cleaning efficacy. The shear stress forces at the membrane surface and the Reynolds numbers within the hollow fiber membranes were calculated for each step of the different physical cleaning strategies considered (Table 3). All Reynolds numbers calculated were in the laminar regime. Air injection during the first forward flush increased the shear stress forces by 2- to 3-fold and both Reynolds number by 4- to 9-fold, compared with those for the single-phase (i.e., water) flow conditions. With air injection, the maximum shear stress and Reynolds numbers were for the forward flush + air (step 1), with the exception of protocol 3, for which the maximum shear stress was for the BW + forward flush (step 2). Without air injection, the maximum values were always during BW + forward flush (step 2). As a reference, the shear stress and Reynolds numbers achieved during CF operation reached 5.0 Pa and 400, respectively. Interestingly, all maximum shear stress calculated during physical cleaning were below this number

while only cleaning protocols with air achieved Reynolds numbers above 400.

A number of parameters have been considered in the past to relate the hydrodynamic conditions present in membrane systems to fouling control [11,12,15,31,32,33]. Most of these attempts to relate a value based on the shear stress present at the surface of a membrane to fouling control [15,31,32,33]. Unfortunately, the accurate determination of shear stress values theoretically or experimentally is very complex. Also, most of the shear stress-based parameters considered to date do not

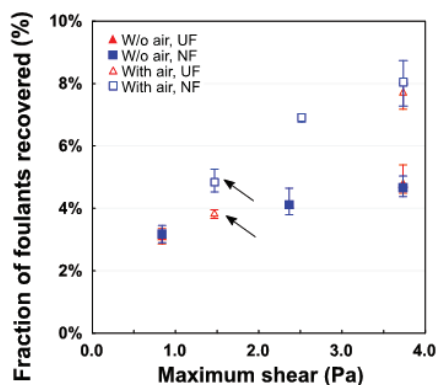
generate a continuous relationships that can be universally applied to all hydrodynamic conditions of interest, especially when considering single-phase and dual-phase flow [34]. This limitation is most likely due to the complexity of the slug flow shear pattern within a tube, which induce a shear with a magnitude and direction, which fluctuates with the passage of bubbles [32]. According to previous studies [33,34], the mean shear stress is not representative of the fluctuations occurring at the fiber wall. This observation also points out to the limitations of using theoretical shear stress calculations and warrants the use of experimental shear stress measurements.

In the present study, the Reynolds number was considered as a simple parameter to relate the hydrodynamic conditions present in a membrane system to fouling control. The best correlation was observed while using the maximum mixture Reynolds number (Re_m) values achieved during a given protocol (Fig. 5(b)), although cleaning efficacy was also correlated with the maximum shear (Fig. 5(a)). Without air addition, the max Re_m ranged from 48 to 135 for the conditions investigated, and a linear relationship was observed between the maximum Re_m and the fraction of foulants recovered. With air addition, the maximum Re_m ranged from 382 to 516 for the conditions investigated. Again, a linear relationship was observed between the maximum Re_m and the fractions of foulants recovered. Unlike the shear stress-based parameters, a continuous relationship was observed between the Re_m and the fraction of foulants recovered for all conditions investigated (linear fitting, $R^2 = 0.72$). The mixture Reynolds number was reported to be proportional to the liquid velocity in the mixture and is also a linear function of the gas slug frequency [31]. It could be a rough indicator to compare physical cleaning protocols without having to rely on filtration experiments. It would be of interest to validate if physical cleaning efficacy can also be predicted with the mixture Reynolds number under other test conditions. In this study case, the fiber diameter was small ($D = 0.8$ mm), and the hydrodynamic was influenced by viscosity (for $D < 50$ (μ^2/ρ^2g)^{1/3} = 2.3 mm) [35], but also controlled by surface tension (for $Eö < 3.37$, $D = 5.0$ mm) [36]. Therefore, it is not expected that the mixture Reynolds number would be applicable to any fiber geometry.

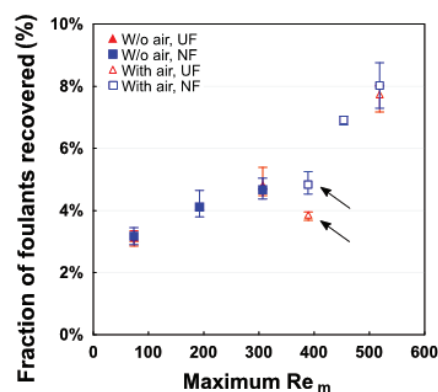
Table 3
Shear stresses and Reynolds numbers achieved during each individual cleaning step

Protocols	Cleaning steps	Shear (Pa)	Re_m
1	Step 1: Forward flush without air (with air)	0.5 (1.5)	48 (382)
	Step 2: Backwash + forward flush	0.8	64
	Step 3: Forward flush without air	0.5	48
2	Step 1: Forward flush without air (with air)	1.1 (2.5)	88 (459)
	Step 2: Backwash + forward flush	2.3	183
	Step 3: Forward flush without air	1.1	88
3	Step 1: Forward flush without air (with air)	1.7 (3.5)	135 (516)
	Step 2: Backwash + forward flush	3.8	303
	Step 3: Forward flush without air	1.7	135

The numbers in parenthesis provide the values for the conditions with air injection.



(a) Fraction of foulants recovered by physical cleaning (%) vs. maximum shear stress (Pa)



(b) Fraction of foulants recovered by physical cleaning (%) vs. maximum Re_m

Fig. 5. Shear and Reynolds number as indicators of physical cleaning efficacy for HFNF and HFUF membranes (flux 20 LMH and CF of 0.5 m/s; error bars provide the min-max deviations). The arrows indicate results for cleaning protocol 1 for which the void ratio was very high (above 0.90).

Table 4
Total energy demand for the various cleaning protocols applied to HFNF

Criteria	Physical cleaning protocols					
	P1	P1 + air	P2	P2 + air	P3	P3 + air
Mean fraction of foulants recovered by PC (%)	3.1	4.3	4.1	6.9	4.7	7.8
Physical cleaning specific energy (W-h/m ³)	3.1	3.2	1.5	1.7	1.9	2.3
Total specific energy demand (W-h/m ³) ¹	209	209	204	204	204	204
Backwash waters (% of production)	3.3	3.3	1.4	1.4	1.4	1.4
Wastewater (m ³ /module)	0.05	0.05	0.05	0.05	0.08	0.08

¹Total energy = Permeation + crossflow + physical cleaning energies.

As expected, higher water velocities and air addition increased the wall shear stress [32]. Dual-phase physical cleaning conditions proved to be superior to single-phase (i.e., water) cleaning. Such observations are consistent with conclusions from previous studies [18,19]. As previously discussed, the maximum mixture Reynolds numbers for the physical cleaning protocols with air addition were achieved during the dual-phase forward flush. For protocols without air addition, it was achieved during the BW with forward flush. For protocol 1 (see arrows in Fig. 5), the impact of air addition on efficacy was less important. This is potentially due to the very high void ratio (0.91) that may have favored an annular flow condition (observed above 0.90) rather than slug flow [33], the latter being more effective for fouling control.

3.4. Energy consumption

The specific energy consumptions (i.e., normalized for one m³ of treated water) were calculated for the different cleaning protocols investigated. The calculations assumed CF operation of a HFNF membrane at 20 LMH (20°C). The protocol P1 had the highest energy consumption (Table 4). This extra energy demand comes from the longer duration (2-fold) for the BW step at high pressure (4.8 bar) compared with those of protocols P2 and P3. The BW alone consumes 55%–74% of the total cleaning energy. Air injection marginally increases the energy cost of the protocols (20%), but achieved a higher physical cleaning efficacy with less energy than water alone.

Although these differences may appear important, they are actually marginal when compared with the total energy cost of operation of a HFNF, which including filtration and CF. For example, the total energy demand in CF are presented in Table 4 for the six cleaning strategies. The cleaning energy of HFNF is negligible compared with that of operation (below 1.5%). The BW step for P1 requires 3.3% of the treated water production for the physical cleaning while P2 and P3 only use 1.4%.

Dual-phase was also shown to be less energy-intensive than water alone to achieve a given physical efficacy. The HFNF membrane is limited to low BW flux due to its lower permeability. Such constraint can be mitigated by the use of air. A shorter BW duration and air addition in the forward flush could provide an enhanced physical cleaning while minimizing operation and maintenance (O&M) costs of physical cleaning. With respect to energy

optimization, the specific energy for the different physical cleaning strategies were in the order of 1.5–3.2 W-h/m³. The contribution of the physical cleaning strategies to the total energy demand (i.e., including CF and permeation energies) is marginal because of the higher operation pressure required for HFNF membranes. Optimizing physical cleaning of HFNF will therefore only provide low relative energy savings.

4. Conclusions

HFNF and HFUF mini-modules of identical dimensions were fouled under DE and CF operation using synthetic waters. Various physical cleaning strategies were assessed to maximize foulant recoveries from the membrane. Experimental results led to the following conclusions:

- There was no significant difference between the physical cleaning efficacy of HFUF and HFNF membranes when operated with CF at a permeation flux typical of HFNF (20 LMH). The use of air, high water velocity or a combination of both improved the physical cleaning efficacy by 2.5-fold compared with low velocity in the absence of air addition.
- Air-assisted forward flush increased the wall shear stress and Reynolds number. Physical cleaning efficacy was best correlated to the maximum mixture Reynolds number (calculated for the cleaning step with the highest velocity).
- Air addition increases energy costs but improves the efficacy of physical cleaning with less energy than water alone and without producing extra wastewaters.
- The benefit of optimizing physical cleaning for HFNF membranes is lower than for HFUF membranes because of the higher pressure of operation and the use of CF operation required for HFNF membranes.

Acknowledgments

The authors would like to thank Joerg Winter (University of British Columbia) for LC-OCD analysis and for some useful discussions on nanofiltration fouling. This study was performed at the CREDEAU laboratory, a CFI research infrastructure of Polytechnique Montreal. The work was supported financially by RES'EAU-WaterNET, an NSERC strategic research network dedicated to providing safe drinking water to small rural communities.

Symbols

α	—	Void fraction
C	—	Chisholm empirical factor
D	—	Fiber inner diameter, m
f_D	—	Darcy friction factor
f_f	—	Friction factor
g	—	Gravitational acceleration, m·s ⁻²
Lo^*	—	Non-dimensional Laplace constant
Re	—	Reynolds number
Re_m	—	Mixture Reynolds number
U_G	—	Gas velocity, m/s
U_L	—	Liquid velocity, m/s
U_m	—	Mixture velocity, m/s
X	—	Empirical parameter
ΔL	—	Fiber length, m
ΔP	—	Pressure loss, Pa
Φ_L^2	—	Multiplier factor
μ_L	—	Liquid dynamic viscosity, Pa·s
μ_m	—	Mixture dynamic viscosity, Pa·s
ρ_G	—	Gas density, kg/m ³
ρ_L	—	Liquid density, kg/m ³
ρ_m	—	Mixture density, kg/m ³
σ	—	Surface tension, N·m ⁻¹
τ_{wall}	—	Wall shear stress, Pa

References

- [1] A.W. Mohammad, Y.H. Teow, W.L. Ang, Y.T. Chung, D.L. Oatley-Radcliffe, N. Hilal, Nanofiltration membranes review: recent advances and future prospects, *Desalination*, 356 (2015) 226–254.
- [2] C. Shankaraman, J.G. Jacangelo, T.P. Bonacquisti, B.A. Schauer, Effect of pretreatment on surface water nanofiltration, *J. Am. Water Works Assoc.*, 89 (1997) 77–89.
- [3] K.H. Chu, S.S. Yoo, Y. Yoon, K.B. Ko, Specific investigation of irreversible membrane fouling in excess of critical flux for irreversibility: a pilot-scale operation for water treatment, *Sep. Purif. Technol.*, 151 (2015) 147–154.
- [4] A.S. Al-Amoudi, Factors affecting natural organic matter (NOM) and scaling fouling in NF membranes: a review, *Desalination*, 259 (2010) 1–10.
- [5] D. Jermann, W. Pronk, S. Meylan, M. Boller, Interplay of different NOM fouling mechanisms during ultrafiltration for drinking water production, *Water Res.*, 41 (2007) 1713–1722.
- [6] C.Y. Tang, Y.-N. Kwon, J.O. Leckie, The role of foulant–foulant electrostatic interaction on limiting flux for RO and NF membranes during humic acid fouling—theoretical basis, experimental evidence, and AFM interaction force measurement, *J. Membr. Sci.*, 326 (2009) 526–532.
- [7] X. Li, J. Li, X. Fang, K. Bakzhan, L. Wang, B. Van der Bruggen, A synergetic analysis method for antifouling behavior investigation on PES ultrafiltration membrane with self-assembled TiO₂ nanoparticles, *J. Colloid Interface Sci.*, 469 (2016) 164–176.
- [8] E.M. Vrijenhoek, S. Hong, M. Elimelech, Influence of membrane surface properties on initial rate of colloidal fouling of reverse osmosis and nanofiltration membranes, *J. Membr. Sci.*, 188 (2001) 115–128.
- [9] Q. She, R. Wang, A.G. Fane, C.Y. Tang, Membrane fouling in osmotically driven membrane processes: a review, *J. Membr. Sci.*, 499 (2016) 201–233.
- [10] S.-H. Yoon, C.-H. Lee, K.-J. Kim, A.G. Fane, Effect of calcium ion on the fouling of nanofilter by humic acid in drinking water production, *Water Res.*, 32 (1998) 2180–2186.
- [11] J.-y. Tian, Y.-p. Xu, Z.-l. Chen, J. Nan, G.-b. Li, Air bubbling for alleviating membrane fouling of immersed hollow-fiber membrane for ultrafiltration of river water, *Desalination*, 260 (2010) 225–230.
- [12] L. Xia, A.W.-K. Law, A.G. Fane, Hydrodynamic effects of air sparging on hollow fiber membranes in a bubble column reactor, *Water Res.*, 47 (2013) 3762–3772.
- [13] Z.F. Cui, K.I.T. Wright, Flux enhancements with gas sparging in downwards crossflow ultrafiltration: performance and mechanism, *J. Membr. Sci.*, 117 (1996) 109–116.
- [14] S. Laborie, C. Cabassud, L. Durand-Bourlier, J.M. Lainé, Flux enhancement by a continuous tangential gas flow in ultrafiltration hollow fibres for drinking water production: effects of slug flow on cake structure, *Filtr. Sep.*, 34 (1997) 887–891.
- [15] Z. Cui, T. Taha, Enhancement of ultrafiltration using gas sparging: a comparison of different membrane modules, *J. Chem. Technol. Biotechnol.*, 78 (2003) 249–253.
- [16] T.W. Cheng, J.G. Wu, Quantitative flux analysis of gas–liquid two-phase ultrafiltration, *Sep. Sci. Technol.*, 38 (2003) 817–835.
- [17] J.Q.J.C. Verberk, J.C. van Dijk, Air sparging in capillary nanofiltration, *J. Membr. Sci.*, 284 (2006) 339–351.
- [18] C. Serra, L. Durand-Bourlier, M.J. Clifton, P. Moulin, J.C. Rouch, P. Aptel, Use of air sparging to improve backwash efficiency in hollow-fiber modules, *J. Membr. Sci.*, 161 (1999) 95–113.
- [19] Y. Bessiere, C. Guigui, P.J. Remize, C. Cabassud, Coupling air-assisted backwash and rinsing steps: a new way to improve ultrafiltration process operation for inside-out hollow fibre modules, *Desalination*, 240 (2009) 71–77.
- [20] P.J. Remize, C. Guigui, C. Cabassud, Evaluation of backwash efficiency, definition of remaining fouling and characterisation of its contribution in irreversible fouling: case of drinking water production by air-assisted ultra-filtration, *J. Membr. Sci.*, 355 (2010) 104–111.
- [21] A. Braghetta, F.A. DiGiano, W.P. Ball, NOM accumulation at NF membrane surface: impact of chemistry and shear, *J. Environ. Eng., ASCE*, 124 (1998) 1087–1098.
- [22] A. Seidel, M. Elimelech, Coupling between chemical and physical interactions in natural organic matter (NOM) fouling of nanofiltration membranes: implications for fouling control, *J. Membr. Sci.*, 203 (2002) 245–255.
- [23] Pentair Ultrafiltration (UF) technology. <http://xflow.pentair.com/en/products/xiga>, Access December 28, 2016.
- [24] F. Holland, R. Bragg, *Fluid Flow for Chemical and Process Engineers*, Butterworth-Heinemann, Elsevier, Amsterdam, The Netherlands, 384 p., ISBN: 9780340610589, 1995.
- [25] F.M. White, *Fluid Mechanics*, McGraw-Hill, 5th edition, New York, NY, USA, 853 p., ISBN: 978-0072402179, 2003.
- [26] R.W. Lockhart, R.C. Martinelli, Proposed correlation of data for isothermal two-phase, two-component flow in pipes, *Chem. Eng. Prog.*, 45 (1949) 39–48.
- [27] D. Chisholm, A theoretical basis for the Lockhart-Martinelli correlation for two-phase flow, *Int. J. Heat Mass Transfer*, 10 (1967) 1767–1778.
- [28] W. Zhang, T. Hibiki, K. Mishima, Correlations of two-phase frictional pressure drop and void fraction in mini-channel, *Int. J. Heat Mass Transfer*, 53 (2010) 453–465.
- [29] N. Hilal, H. Al-Zoubi, N.A. Darwish, A.W. Mohamma, M. Abu Arabi, A comprehensive review of nanofiltration membranes: treatment, pretreatment, modelling, and atomic force microscopy, *Desalination*, 170 (2004) 281–308.
- [30] J. Winter, P.R. Bérubé, NF-UF range membranes for drinking water treatment, *British Columbia Water and Waste Association Annual Conference*, Keylowna, BC, 2015.
- [31] S. Laborie, C. Cabassud, L. Durand-Bourlier, J.M. Lainé, Characterisation of gas–liquid two-phase flow inside capillaries, *Chem. Eng. Sci.*, 54 (1999) 5723–5735.
- [32] N. Ratkovich, P.R. Berube, I. Nopens, Assessment of mass transfer coefficients in coalescing slug flow in vertical pipes and applications to tubular airlift membrane bioreactors, *Chem. Eng. Sci.*, 66 (2011) 1254–1268.
- [33] C. Cabassud, S. Laborie, L. Durand-Bourlier, J.M. Lainé, Air sparging in ultrafiltration hollow fibres: relationship between flux enhancement, cake characteristics and hydrodynamic parameters, *J. Membr. Sci.*, 181 (2001) 57–69.
- [34] C.C.V. Chan, P.R. Bérubé, E.R. Hall, Relationship between types of surface shear stress profiles and membrane fouling, *Water Res.*, 45 (2011) 6403–6416.
- [35] G.B. Wallis, *One-dimensional Two-phase Flow*, McGraw-Hill, New York, 1969.
- [36] F.P. Bretherton, The motion of long bubbles in tubes, *J. Fluid Mech.*, 10 (1961) 166–188.